© 2018. Published by The Company of Biologists Ltd | Journal of Cell Science (2018) 131, jcs224204. doi:10.1242/jcs.224204

CORRECTION

Correction: Migration against the direction of flow is LFA-1-dependent in human hematopoietic stem and progenitor cells (doi: 10.1242/jcs.205575)

Alexander Buffone, Jr, Nicholas R. Anderson and Daniel A. Hammer

There was an error published in *J. Cell Sci.* (2018) **131**, jcs205575 (doi: 10.1242/jcs.205575).

In Movie 8, the direction of flow was labelled incorrectly. Movie 8 has now been replaced with the correct version. There are no changes to the movie legend, which is accurate.

The authors would like to apologise to readers for this error.

© 2018. Published by The Company of Biologists Ltd | Journal of Cell Science (2018) 131, jcs205575. doi:10.1242/jcs.205575

RESEARCH ARTICLE

Migration against the direction of flow is LFA-1-dependent in human hematopoietic stem and progenitor cells

Alexander Buffone, Jr[1], Nicholas R. Anderson[1] and Daniel A. Hammer[1,2,*]

ABSTRACT

The recruitment of immune cells during inflammation is regulated by a multi-step cascade of cell rolling, activation, adhesion and transmigration through the endothelial barrier. Similarly, hematopoietic stem and progenitor cells (HSPCs) use this pathway to migrate and home to the bone marrow. After selectin-mediated braking, HSPCs migrate on adhesion ligands presented by the vascular endothelium including ICAM-1, VCAM-1 or MAdCAM-1. Here, we report that both the KG1a stem cell line and primary bone marrow CD34$^+$ HSPCs can migrate against the direction of fluid flow on surfaces coated with cell adhesion molecules (CAMs), a behavior thus far only reported in T lymphocytes. We demonstrate that KG1a cells and primary HSPCs migrate upstream on surfaces presenting ICAM-1, downstream on surfaces presenting VCAM-1, and both upstream and downstream on surfaces presenting MAdCAM-1. In addition, we demonstrate that KG1a cells and HSPCs display upstream migration both on surfaces with multiple CAMs, as well as on human umbilical vein endothelial cell (HUVEC) monolayers. By blocking with monoclonal antibodies, we show that lymphocyte function-associated antigen-1 (LFA-1) is the key receptor responsible for upstream migration on the endothelium during the trafficking of HSPCs to the bone marrow.

This article has an associated First Person interview with the first author of the paper.

KEY WORDS: Hematopoietic stem and progenitor cell, Inflammation, ICAM-1, VCAM-1, MAdCAM-1, Cell migration, LFA-1, Endothelium, Homing

INTRODUCTION

Immune cell recruitment to sites of inflammation is mediated by a multistep process known as the leukocyte adhesion cascade. Initially, cells are slowed by selectin-mediated interactions, allowing for chemokine-induced activation of integrins and resulting firm adhesion, which eventually leads to transmigration across the endothelial layer (Ley et al., 2007; Springer, 1994). Hematopoietic stem and progenitor cells (HSPCs), which are a heterogeneous population of cells defined by the molecular expression of CD34 (CD34$^+$), include long-term and short-term stem cells, multipotent progenitor cells and lineage-restricted myeloid and lymphoid progenitors (Carvalho et al., 2009). These cells reside in the bone marrow and give rise to all end-effector immune cells. HSPCs use the leukocyte adhesion cascade to home back to the bone marrow and re-establish normal hematopoiesis post transplantation (Appelbaum, 2007). In the first step of the adhesion cascade, human HSPCs bind and roll on all three (E-, P- and L-) selectins (Greenberg et al., 2000), but principally interact with E-selectin on the surface of the microvasculature through a specific sialyl-lewis X (sLe^X)-decorated glycoform of CD44 termed HCELL (Dimitroff et al., 2001a; Sackstein and Dimitroff, 2000). Adhesion can also be mediated by P-selectin glycoprotein ligand-1 (PSGL-1; also known as SELPLG) on the HSPC surface. Upon E-selectin-mediated braking, intracellular signaling cascades are activated in HSPCs by endothelium-bound CXCL12 through its cognate cell surface receptor CXCR4 (Peled et al., 1999b; Schweitzer et al., 1996). These cascades trigger cell-borne integrins, such as VLA-4 ($\alpha_4\beta_1$) and LFA-1 ($\alpha_L\beta_2$), to adopt high affinity states which lead to arrest on the apical surface of endothelium. Once stopped, cells can begin to migrate along surfaces presenting cellular adhesion molecules (CAMs) (Huttenlocher and Horwitz, 2011; Peled et al., 1999a), principally VCAM-1 and ICAM-1, which are distributed broadly (Schweitzer et al., 1996) but are specifically expressed at high levels on the bone marrow endothelium (Papayannopoulou et al., 1995). This tight binding and firm arrest then leads to subsequent diapedesis through the endothelium to reach the basal lamina. HSPCs must migrate through this space to reach the bone marrow (Sahin and Buitenhuis, 2012) and restart hematopoiesis.

Previous work by ourselves and others has demonstrated an interesting phenomena where both murine and human T lymphocytes can migrate efficiently upstream (against the direction of shear-flow) on surfaces presenting ICAM-1 and ICAM-2, while migrating downstream (with the direction of shear flow) on surfaces presenting VCAM-1 (Steiner et al., 2010). Other immune cell types, such as neutrophils, do not demonstrate upstream migration (Dominguez et al., 2015; Valignat et al., 2013). On surfaces presenting both VCAM-1 and ICAM-1, T cells also migrate upstream (Dominguez et al., 2015). Furthermore, the efficiency of the upstream migration is dependent on the shear rate, as increasing the shear rate results in increased upstream migration of T-cells on ICAM-1-presenting surfaces (Dominguez et al., 2015; Valignat et al., 2013). Since HSPCs have similar cell surface integrin receptor profiles to T-lymphocytes [such as VLA-4, LFA-1 and $\alpha_X\beta_2$ (Chan and Watt, 2001)], it was natural to ask whether HSPCs display upstream migration on surfaces presenting ICAM-1. Like T-cells, HSPCs would have the capability to bind to both VCAM-1 and ICAM-1, and should be candidates for upstream migration due to their expression of β_2 integrins. HSPCs also express LPAM-1 ($\alpha_4\beta_7$), which is the principal ligand for MAdCAM-1 (Berlin et al., 1993) which has been implicated as working in concert with VLA-4 in the homing of HSPCs to the bone marrow in mice (Katayama et al., 2004).

Our study sought to determine whether upstream migration under fluid flow could be seen in HSPCs. We used both a human cell line,

[1]Departments of Chemical and Biomolecular Engineering, University of Pennsylvania, Philadelphia, PA 19104, USA. [2]Bioengineering, University of Pennsylvania, Philadelphia, PA 19104, USA.

*Author for correspondence (hammer@seas.upenn.edu)

D.A.H., 0000-0002-3522-3154

Received 26 April 2017; Accepted 20 November 2017

Journal of Cell Science (2018) 131, jcs205575. doi:10.1242/jcs.205575

KG1a cells, which have been previously used as a model for HSPCs (Dimitroff et al., 2001a,b; She et al., 2012), and primary bone marrow-derived HSPCs. Our results demonstrate that both KG1a cells and HSPCs migrate upstream in an LFA-1-dependent manner on surfaces presenting ICAM-1 or MAdCAM-1, and mixed surfaces containing ICAM-1, as well as on activated endothelial monolayers. These results imply that LFA-1 engagement is indispensable for the upstream direction of stem cells, which facilitates HSPC migration to specific sites to enter the bone marrow.

RESULTS

KG1a cells are HSPC-like, express receptor ligands for, and are motile on ICAM-1, VCAM-1 and MAdCAM-1

The KG1a cell line is a human hematopoietic cell line that expresses similar numbers of the surface marker CD34 to bone marrow-derived HSPCs (Fig. S1), making them an excellent model cell line for HSPCs. We performed flow cytometry to determine what cell-borne receptors for CAMs are expressed on the surface of KG1a cells and bone marrow HSPCs (Fig. 1). Flow cytometry revealed that KG1a cells express the α_L, α_4 and α_5 integrin subunits at high levels, have moderate expression of α_X, and show no expression of α_M (Fig. 1A). In addition, KG1a cells expressed high levels of β_1 and β_2 integrin subunits and low expression of β_7 (Fig. 1B). The primary bone marrow HSPCs expressed all of the α (Fig. 1C) and β integrin subunits (Fig. 1D), albeit at lower levels than KG1a cells. Taken together, KG1a cells and HSPCs express the integrin heterodimers LFA-1 ($\alpha_L\beta_2$), $\alpha_X\beta_2$, VLA-4 ($\alpha_4\beta_1$), VLA-5 ($\alpha_5\beta_1$) and LPAM-1 ($\alpha_4\beta_7$), while being negative for MAC-1 ($\alpha_M\beta_2$). Expression of these cell surface integrins suggests that KG1a cells have the ability to migrate on ICAM-1, VCAM-1 and MAdCAM-1 surfaces.

We measured the motility of KG1a cells on substrates coated with endothelial CAMs in the absence of flow at a fixed concentration of 2.5 µg/ml. In the traces presented in the figures tracking the path of migration, blue represents rightward migration (with the flow) and red indicates leftward migration (against the flow). Fig. 2 illustrates the motion of KG1a cells on VCAM-1 (Fig. 2A), ICAM-1 (Fig. 2B) and MAdCAM-1 (Fig. 2C) surfaces. The migration index (MI) fell between −0.05 and 0.05 for all three CAMs, indicating that in the absence of flow, there is no preference in direction of migration. The two-dimensional area KG1a cells explored through migration in the same period of time was different on each CAM surface and followed the trend VCAM-1<ICAM-1<MAdCAM-1. The persistence time (Fig. 2D) of KG1a cells on ICAM-1 (6.79±1.36 min; mean±s.e.m.) was slightly less than that of VCAM-1 (8.64±1.51 min), but both were significantly lower than on MAdCAM-1 (15.2±2.48 min). The speed (Fig. 2E) of KG1a cells on VCAM-1 (4.71±0.37 µm/min) was significantly slower than on ICAM-1 (7.44±1.18 µm/min), which was in turn significantly slower than on MAdCAM-1 (10.5±1.21 µm/min). The random motility coefficient (Fig. 2F), which is an overall measure of the motility, was also lower on VCAM-1 (90.4±8.1 μm^2/min), than on ICAM-1 (175.1±29.4 μm^2/min), which was less than on MAdCAM-1 (589.4±91.8 μm^2/min). Thus, KG1a cells are motile on each CAM surface.

KG1a cells migrate upstream on ICAM-1 surfaces, downstream on VCAM-1 surfaces, and bi-directionally on MAdCAM-1 surfaces under shear flow

Next, we studied the motility of KG1a cells on ICAM-1, VCAM-1 and MAdCAM-1 under shear flow at both a lower shear rate (100 s^{-1}) and a higher shear rate (800 s^{-1}) (Fig. 3). On ICAM-1 surfaces, KG1a cells have a slight preference for upstream migration at low shear rates (Fig. 3A, middle) and a strong preference for upstream migration at high shear rates (Fig. 3A, right; Movie 1). The directional preference was quantified through the MI (Fig. 3D), which decreases (with more negative values indicating more persistent upstream motion) with increasing shear rate from −0.18±0.01 at 100 s^{-1} to −0.37±0.04 at 800 s^{-1} (mean±s.e.m.). On VCAM-1 surfaces, KG1a cells have a strong preference for downstream migration at both low (Fig. 3B, middle) and high shear rates (Fig. 3B, right; Movie 2). This preference is also seen in the MI (Fig. 3D), which increases with increasing shear rate from 0.6±0.03 at 100 s^{-1} to 0.71±0.02 at 800 s^{-1}. Taken together, these data demonstrate that KG1a cells migrate more avidly against direction of flow with increasing shear rate on ICAM-1 surfaces, while migrating with the direction of flow on VCAM-1 surfaces. This phenotype has only been previously seen with T lymphocytes,

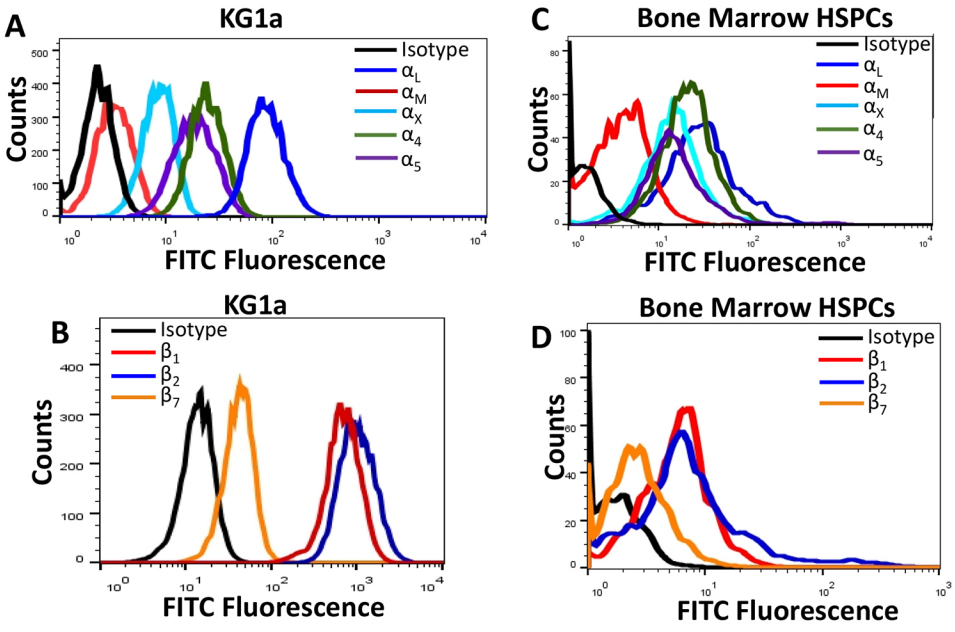

Fig. 1. Expression of integrin subunits on KG1a cells and primary bone marrow HSPCs. 10^5 KG1a cells were assayed for expression of (A,C) integrin α chains and (B,D) integrin β chains. Expression of integrins α_L (dark blue), α_M (red), α_X (light blue), α_4 (green) and α_5 (purple) on (A) KG1a cells and (C) primary bone marrow HSPCs. Expression of integrins β_1 (red), β_2 (light blue) and β_7 (yellow) on (B) KG1a cells and (D) primary bone marrow HSPCs. Isotype controls are depicted in black. In summary, these data show KG1a cells and bone marrow HPSCs express the cell-borne integrins LFA-1, VLA-4, VLA-5, LPAM-1 and $\alpha_X\beta_2$ but not Mac-1.

Journal of Cell Science (2018) 131, jcs205575. doi:10.1242/jcs.205575

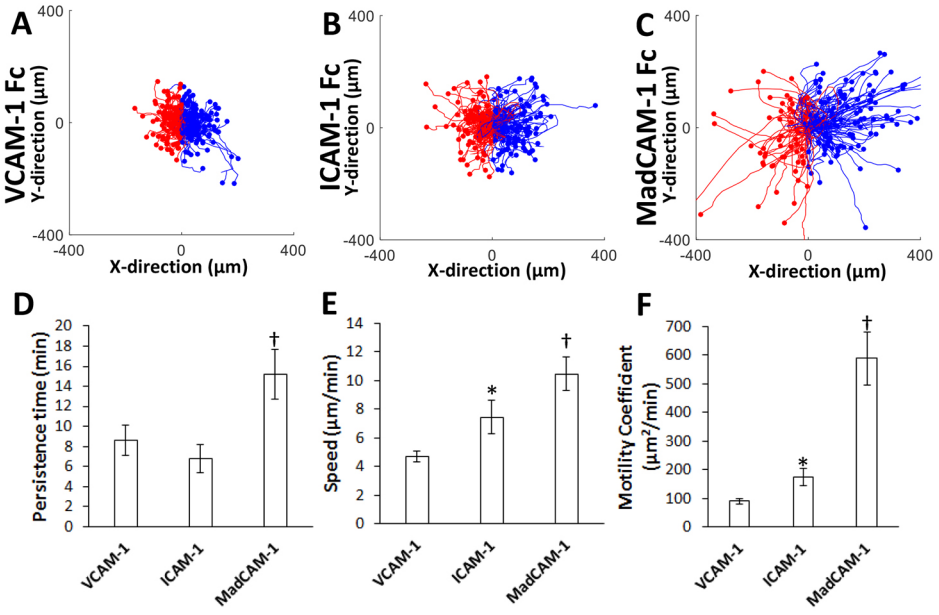

Fig. 2. Motility on CAM surfaces under static conditions. Cell traces of KG1a cells under static conditions on (A) VCAM-1, (B) ICAM-1 and (C) MAdCAM-1 at a concentration of 2.5 μg/ml. The traces depicted are the cumulative tracks of three independent experiments and have units of μm. Blue traces indicate cells that traveled to the right while red traces indicate cells that traveled to the left. KG1a cells migrating along each of the three CAM surfaces had an MI of –0.05<MI<0.05 indicating random motility. In general, the area explored by KG1a in the traces follow the pattern VCAM-1<ICAM-1<MAdCAM-1. The (D) persistence time (min), (E) speed (μm/min) and (F) random motility coefficient (μm^2/min) were calculated for each CAM. In all, KG1a cells the motility and speed followed the trend VCAM-1<ICAM-1<MAdCAM-1 (n=4 independent experiments of at least 70 cells analyzed per experiment for each CAM). *P<0.05 with respect to VCAM-1; †P<0.05 with respect to all other CAMs (one-way ANOVA).

so this observation has now been extended to an important new cell type.

MAdCAM-1 has not been previously studied for its propensity to direct directional migration under flow. On MAdCAM-1 surfaces, the cell tracks illustrate that the KG1a cells have a bi-directional motion at both low (Fig. 3C, middle) and high (Fig. 3C, right; Movie 3) shear rates. This bi-directional motion is caused by a distinct subpopulation of cells that migrate upstream, while the majority of cells migrate downstream. The MI (Fig. 3D) only slightly increases with increasing shear rate, from 0.22±0.05 at 100 s^{-1} and to 0.29±0.05 at 800 s^{-1}. For all three CAMs, the speed and persistence time of migration showed no dependence on shear rate (Fig. S2).

LFA-1 controls the upstream migration in KG1a cells on ICAM-1 and MAdCAM-1

To understand the role of integrins in the directional motion of KG1a cells under shear flow, we measured both the directional motion and amount of adhesion of KG1a cells on ICAM-1, VCAM-1 and MAdCAM-1 surfaces under high shear rates (800 s^{-1}) in the presence of blocking antibodies against specific cell-borne integrins (Fig. 4).

In the presence of an isotype control antibody, KG1a cells crawl upstream under shear flow on ICAM-1 surfaces (Fig. 4A, left; Movie 4). The binding to ICAM-1 was shown to be β_2 integrin dependent, as an antibody blocking the CD18 subunit reduced adhesion from 73.2±8.5 cells/mm^2 (for the isotype positive control; mean±s.e.m.) to 1.1±0.3 cells/mm^2 (Fig. 4D). By using antibodies, we further investigated the role of different β_2 integrin subunits in adhesion and migration under flow. With an antibody that blocks the CD11a subunit (α_L, LFA-1), migration switches from upstream to downstream (Fig. 4A, middle; Movie 5), while blocking the CD11c subunit (α_X) preserved upstream migration (Fig. 4A, right). Furthermore, while blocking CD11a produced only a marginal reduction in adhesion (62.2±10.9 cells/mm^2), blocking the CD11c subunit almost completely removed adhesion to ICAM-1 (Fig. 4D). The reversal of migration through blocking CD11a was quantified by determining the MI (Fig. 4G), which switches from a negative value of −0.25±0.04 to a positive value of 0.33±0.03. Blocking CD11c does not affect the MI (−0.27±0.08). The MI could not be calculated when CD18 was blocked because so few cells bound to the surface. In summary, LFA-1 controls the upstream motion of KG1a cells on ICAM-1 while the $\alpha_X\beta_2$ integrin is important for adhesion to the surface.

As seen from the cell tracks (Fig. 4B) and MI (Fig. 4H) on VCAM-1 surfaces, KG1a cells migrate downstream (left plot) in the isotype control and the direction of motion was unchanged for all blocking conditions. Binding to VCAM-1 surfaces was shown to be mostly β_1 integrin dependent, with a partial role for β_7 integrins, as blocking β_1 (CD29) reduced adhesion by ∼85% while blocking β_1 and β_7 in combination completely abolished adhesion. In addition, blocking the α_4 chain (CD49d) reduced adhesion ∼95%; this antibody would block the α chains of both VLA-4 ($\alpha_4\beta_1$) and LPAM-1 ($\alpha_4\beta_7$) (Fig. 4E). The MI (Fig. 4H) could not be calculated when β_1 and β_7 together or α_4 were blocked because so few cells were bound. Taken together, the data support the idea that VLA-4 controls the majority of adhesion of KG1a cells to VCAM-1 with the remainder controlled by LPAM-1.

KG1a cells retain their unique bi-directional motion on MAdCAM-1 surfaces upon blocking with an isotype control antibody (Fig. 4C, left). Blocking of L-selectin (CD62L, also known as SELL), a ligand for MAdCAM-1 which is expressed by KG1a cells (data not shown), did not affect either the adhesion to the surface (Fig. 4F) or the MI (Fig. 4I). Adhesion to MAdCAM-1 was β_7 integrin dependent, as blocking LPAM-1 abolished adhesion (Fig. 4F), preventing the calculation of the MI (Fig. 4I). Interestingly, blocking the CD11a chain (LFA-1) did not affect the adhesion to MAdCAM-1 (Fig. 4F) but instead changed the migration from bi-directional to completely downstream (Fig. 4C, middle and right panels, respectively). This change was also reflected in the MI (Fig. 4I), which increased from 0.27±0.02 to 0.74±0.04 upon blocking CD11a at a shear rate of 800 s^{-1}. Taken together, the data suggest that while LPAM-1 controls the adhesion, LFA-1 exclusively controls the upstream motion of KG1a cells on MAdCAM-1.

LFA-1 controls the upstream motion of KG1a on mixed surfaces

To determine whether KG1a cells were able to migrate upstream when more than one CAM was present (as the cell would encounter

Journal of Cell Science (2018) 131, jcs205575. doi:10.1242/jcs.205575

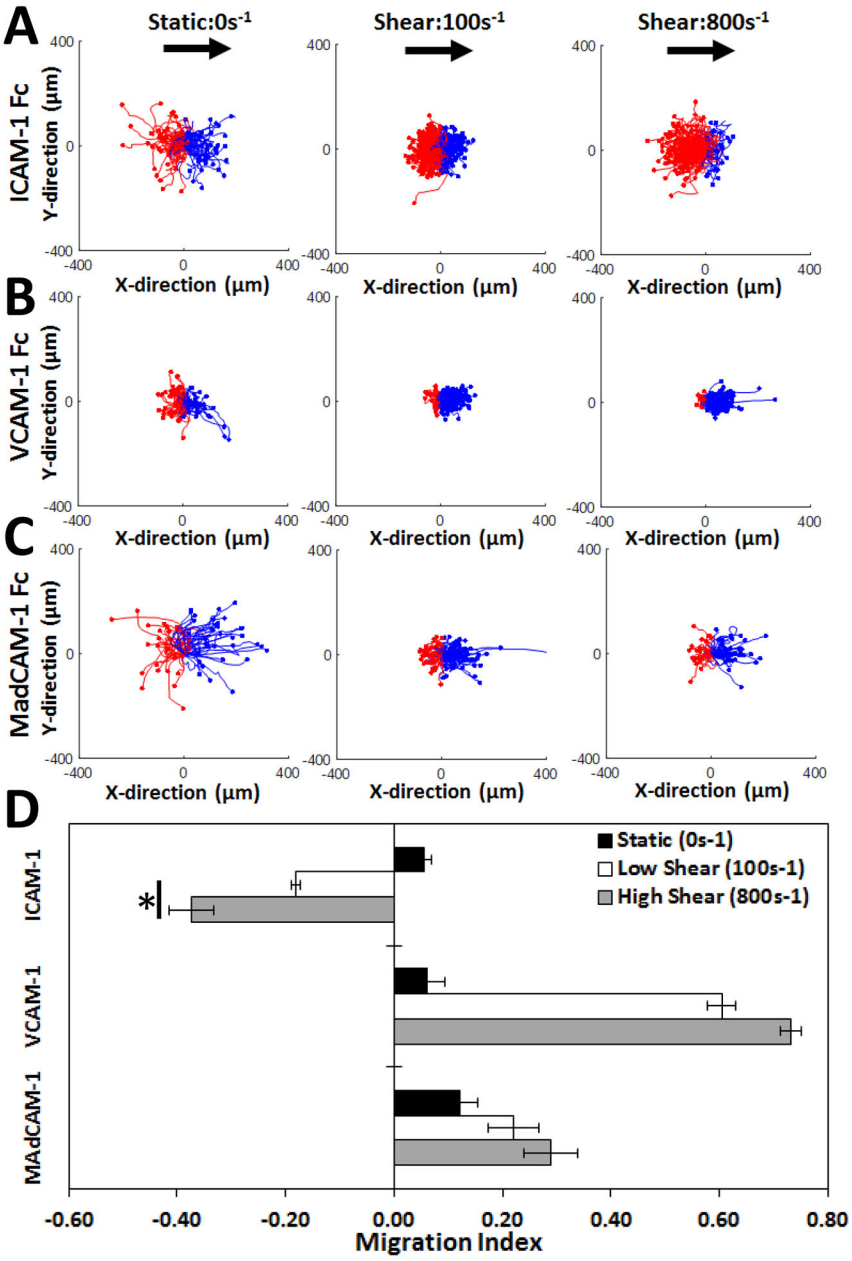

Fig. 3. KG1a cells migrate upstream on ICAM-1, downstream on VCAM-1, and bi-directionally on MAdCAM-1. Cell traces of KG1A cells on (A) ICAM-1, (B) VCAM-1 and (C) MAdCAM-1 under static conditions (first column), at a shear rate of 100 s^{-1} (second column) or at a shear rate of 800 s^{-1} (third column), with a concentration of each adhesion molecule at 5 µg/ml. The traces depicted are the cumulative tracks of three independent experiments and have units of µm. Blue traces indicate cells that traveled downstream (with flow), while red traces indicate cells that traveled upstream (against flow). The direction of flow is from left to right. In general, more of the cell traces indicate upstream motion on ICAM-1 and downstream motion on VCAM-1, while motion is bi-directional on MAdCAM-1. (D) The direction of KG1a cells under shear flow as determined through the MI. A negative MI indicates migration against the flow (upstream), while a positive MI indicates migration with the flow (downstream). KG1a cells migrate upstream on ICAM-1 and this migration increases with shear rate, while KG1a cells migrate downstream on VCAM-1 surfaces and slightly downstream on MAdCAM-1 surfaces independently of shear rate. Results are mean±s.e.m. n=4–5 independent experiments of at least 60 cells analyzed per experiment for each CAM. *P<0.05 with respect to 100 s^{-1} shear rate (one-way ANOVA).

on the endothelial surface), we plated KG1a cells on 50:50 mixtures of both VCAM-1 and ICAM-1 (V_{50}+I_{50}), and ICAM-1 and MAdCAM-1 (I_{50}+M_{50}). As seen in the cell tracks (Fig. 5A,B), upstream migration was seen on both V_{50}+I_{50} and I_{50}+M_{50} surfaces, but with quantitative differences. The MI (Fig. 5C) and the percentage of cells migrating upstream (Fig. 5D) quantifies these differences, indicating that KG1a cells more readily migrate upstream on I_{50}+M_{50} surfaces than on V_{50}+I_{50} surfaces. At a shear rate of 800 s^{-1}, the overall MI is upstream on I_{50}+M_{50} surfaces (−0.14) with 64% of cells migrating upstream, and downstream on V_{50}+I_{50} surfaces (0.33) with only 32% of cells migrating upstream. Next, we demonstrated that blocking the α_L-integrin (CD11a) eliminates upstream migration on mixed surfaces, as illustrated by the lack of red traces after blocking CD11a on either V_{50}+I_{50} and I_{50}+M_{50} surfaces (Fig. 5A,B) and the corresponding increase in MI (Fig. 5C) from 0.33 to 0.62 on V_{50}+I_{50} surfaces and from −0.14 to 0.32 on I_{50}+M_{50} surfaces. The proportion of cells migrating upstream (Fig. 5D) was also reduced to 6.6% and 17.7% on V_{50}+I_{50} surfaces and I_{50}+M_{50} surfaces, respectively. Finally, we demonstrated that blocking the α_4 integrin (CD49d) enhances upstream migration on mixed surfaces, as illustrated by the abundance of red traces after blocking on either V_{50}+I_{50} and I_{50}+M_{50} surfaces (Fig. 5A,B) and the subsequent decrease in MI (Fig. 5C) from 0.33 to −0.28 on V_{50}+I_{50} surfaces (with net migration switching from downstream to upstream) and from −0.14 to −0.33 on I_{50}+M_{50} surfaces. When blocking the α_4 integrin, the proportion of cells migrating upstream (Fig. 5D) increased to 75.6% and 82.9% on V_{50}+I_{50} and I_{50}+M_{50} surfaces, respectively.

We next varied the ratio of VCAM-1 to ICAM-1 (Fig. 5E) or ICAM-1 to MAdCAM-1 (Fig. 5F) while maintaining a constant total concentration of adhesion molecules at 5 µg/ml. This was done to determine which CAM controlled the directional preference cell migration. On surfaces made from VCAM-1 and ICAM-1 (V_x+I_x, where x is the proportion of each molecule as a percentage), KG1a

Journal of Cell Science (2018) 131, jcs205575. doi:10.1242/jcs.205575

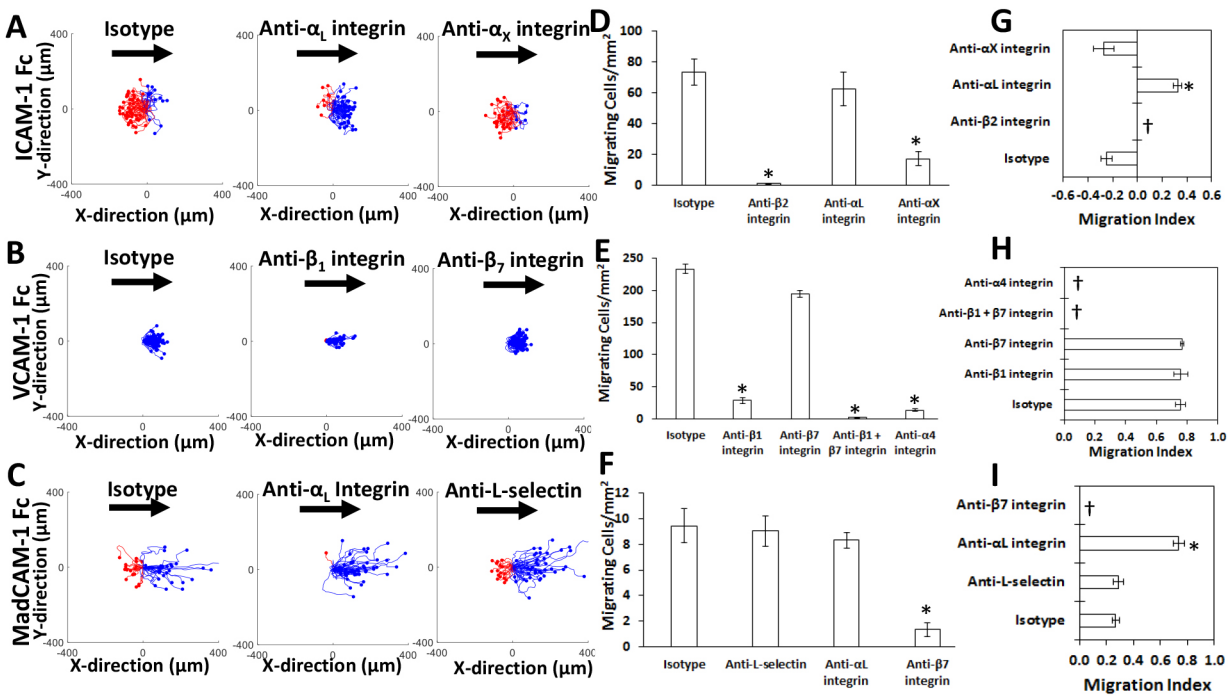

Fig. 4. LFA-1 controls upstream motion while other integrins control adhesion to ICAM-1, VCAM-1 and MAdCAM-1. Cell traces of KG1a cells on (A) ICAM-1, (B) VCAM-1 and (C) MAdCAM-1 surfaces at a 800 s^{-1} shear rate and a ligand concentration of 5 µg/ml in response to blocking antibodies against various cell-borne ligands. The traces are the cumulative tracks of three independent experiments and have units of µm. The direction of flow is from left to right. Blocking β_2 integrins (CD18) or LFA-1 (CD11a) removes the upstream motion of KG1a cells on both ICAM-1 and MAdCAM-1 surfaces. (D–F) The number of migrating cells per mm^2 was calculated for each CAM. In general, adhesion to (D) ICAM-1 was β_2 integrin dependent, (E) VCAM-1 was primarily β_1 integrin dependent and (F) MAdCAM-1 was β_7 integrin dependent. Blocking LFA-1 (CD11a) had no significant effect on number of adhesive cells. MIs for KG1a cells on (G) ICAM-1, (H) VCAM-1 and (I) MAdCAM-1. A negative MI indicates migration against the flow (upstream) while a positive MI indicates migration with the flow (downstream). Empty bars indicate samples in which too few cells adhered to the surface to calculate a MI. Blocking LFA-1 (CD11a) on ICAM-1 or MAdCAM-1 changes the MI of KG1a cells to flow from upstream or bi-directionally to completely downstream. n=4 independent experiments of at least 30 cells analyzed per experiment for each CAM. *P<0.05 with respect isotype control (one-way ANOVA); † indicates conditions with too few adherent cells were present to calculate a MI.

cells prefer to migrate downstream when even 10% VCAM-1 is present. The cell traces (Fig. S3A) and MI (Fig. 5E) show that on ICAM-1 surfaces (V_0+I_{100}), KG1a cells migrate against the direction of flow (MI=−0.30 at 800 s^{-1}), while on 10% VCAM-1 surfaces (V_{10}+I_{90}), KG1a cells migrate downstream, with a net MI of 0.15 at a shear rate of 800 s^{-1}. The preference for downstream migration increases with increasing VCAM-1 concentration (Fig. S3A) and shear rate (Fig. 5E).

Similarly, migration experiments on ICAM-1 to MAdCAM-1 (I_x+M_x, where x is the proportion of each molecule as a percentage) surfaces demonstrate that for KG1a cells, ICAM-1 dominates the directional preference in the absence of VCAM-1. The cell traces (Fig. S3B) and MI (Fig. 5F) show that while a purely MAdCAM-1 surface (I_0+M_{100}) supports bi-directional migration (MI=0.26 at 800 s^{-1}), introducing 25% ICAM-1 (I_{25}+M_{75}) leads to net upstream migration (MI=−0.08 at 800 s^{-1}). The MI then decreases (indicating increased upstream migration) with an increasing proportion of ICAM-1. For all ICAM-1 and MAdCAM-1 mixtures, increasing the shear rate results in more upstream motility.

Taken together, this data shows that KG1a cells can migrate against the direction of flow on surfaces of mixed composition, while the direction of motion under shear flow is determined by VCAM-1>ICAM-1>MAdCAM-1. Furthermore, LFA-1 is the critical receptor mediating upstream motion on surfaces of mixed composition.

Primary bone marrow HSPCs also migrate against the direction of shear flow and demonstrate similar directional preferences to KG1a cells on mixed surfaces

We considered whether the behavior of the immortalized $CD34^+$ KG1a cell line could be extended to primary $CD34^+$ HSPCs from bone marrow (Fig. 6). Primary HSPCs migrate against the direction of flow on ICAM-1 surfaces (Fig. 6A, left panel; Movie 6). The direction of motility was reversed upon blocking the α_L integrin (Fig. 6A, right panel). The directionality was quantified with the MI (Fig. 6B), which decreases with increasing shear rate, from −0.05 at 100 s^{-1} to −0.14 at 800 s^{-1}, indicating increased upstream migration with 60.8% and 65.2% of cells migrating upstream, respectively (Fig. 6C). Furthermore, the direction of motion can be switched to downstream by blocking LFA-1 (MI=0.38 at 100 s^{-1} and 0.39 at 800 s^{-1}).

Fig. 6D illustrates that, on MAdCAM-1 surfaces, HSPCs exhibit the same bi-directional motion previously seen with KG1a cells (left plot). This bi-directional motion is illustrated by the MI (Fig. 6E), which only slightly increases with increasing shear rate, from 0.24 at 100 s^{-1} to 0.30 at 800 s^{-1} with ∼31% of isotype cells migrating upstream at both shear rates (Fig. 6F). Blocking LFA-1 again removes most upstream migration (right plot, Fig. 6D) as downstream motion can be induced by blocking the α_L integrin (MI=0.66 at 100 s^{-1} and 0.79 at 800 s^{-1}) with only 2.1% and 2.6% of cells migrating upstream, respectively.

Journal of Cell Science (2018) 131, jcs205575. doi:10.1242/jcs.205575

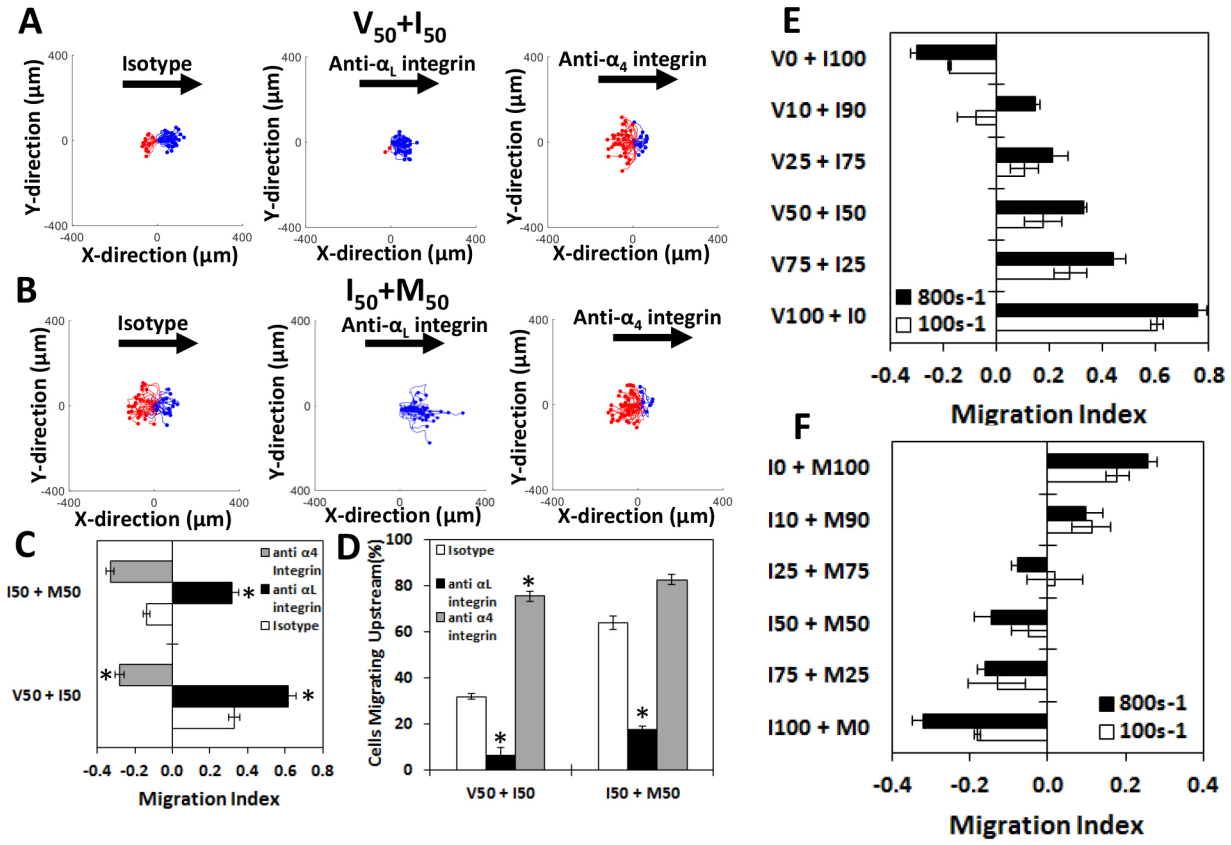

Fig. 5. KG1a cells migrate upstream on mixed CAM surfaces to varying degrees. Cell traces of KG1a cells on (A) V_{50}+I_{50} surfaces and on (B) I_{50}+M_{50} surfaces, and (C) MI and (D) percentage of cells migrating upstream on these surfaces at a shear rate of 800 s^{-1}. Cells migrate downstream on V_{50}+I_{50} and upstream on I_{50}+M_{50} surfaces. Blocking α_L integrin of removes all upstream migration while blocking the α_4 integrin promotes more robust upstream migration on V_{50}+I_{50} and I_{50}+M_{50} surfaces. MI values for KG1a cells on (E) VCAM-1+ICAM-1 and (F) ICAM-1+MAdCAM-1. A negative MI indicates migration against the flow (upstream), while a positive MI indicates migration with the flow (downstream). In general, KG1a cells migrate downstream once any VCAM-1 is introduced in VCAM-1+ICAM-1 mixtures, while they prefer to travel upstream once any ICAM-1 is introduced in ICAM-1+MAdCAM-1 mixtures. *n*=4 independent experiments of at least 40 cells analyzed per experiment for each CAM. **P*<0.05 with respect to isotype control (one-way ANOVA).

On VCAM-1 surfaces, HSPCs migrate downstream (Fig. 6G, left plot; Movie 7), and this is unchanged upon blocking the α_L integrin (right plot). Cells treated with isotype-matched control antibody migrate downstream with a MI of 0.69 at 100 s^{-1} and 0.71 at 800 s^{-1} (Fig. 6H). Blocking the α_L integrin in HSPCs did not significantly change the direction of migration on VCAM-1 (MI=0.60 at 100 s^{-1} and 0.66 at 800 s^{-1}). No HSPCs were seen migrating upstream on VCAM-1 under any of the conditions. Taken together, this data demonstrates that HSPCs migrate with the direction of flow on VCAM-1, independent of shear rate.

Furthermore, on equal mixtures of VCAM-1 and ICAM-1 (Fig. 7A–C) and ICAM-1 and MAdCAM-1 (Fig. 7D–F), HSPCs demonstrate the same directional preferences as KG1a cells (Fig. 7A, left panel). Downstream motion was observed and ∼31% of cells migrated upstream (Fig. 7C) on VCAM-1 and ICAM-1 surfaces. Net upstream motion was observed on ICAM-1+MAdCAM-1 surfaces (Fig. 7D, left panel) with ∼60% of cells traveling upstream at both 100 s^{-1} and 800 s^{-1} (Fig. 7F). Blocking LFA-1 when HSPCs were on mixed VCAM-1+ICAM-1 surfaces (Fig. 7A, middle panel) or on ICAM-1+MAdCAM-1 surfaces (Fig. 7D, right panel) removes all upstream migration. Migration on a surface combining VCAM-1+ICAM-1 (Fig. 7B) gives an MI of 0.24 at 100 s^{-1} and 0.29 at 800 s^{-1} under isotype conditions, and the MI increases to 0.77 at 100 s^{-1} and 0.76 at 800 s^{-1} upon blocking LFA-1. In contrast, blocking VLA-4 on a surface with VCAM-1+ICAM-1 (Fig. 7A, right panel) enhances upstream migration to the point that the net migration switches from downstream to upstream, with >50% of cells traveling upstream. On surfaces of ICAM-1+MAdCAM-1, blocking LFA-1 changes the direction of migration from upstream to downstream. Migration on a surfaces made of ICAM-1+MAdCAM-1 (Fig. 7E) also switches direction upon blocking LFA-1; the MI changes from −0.12 at to 0.64 at 100 s^{-1} and from −0.14 to 0.66 at 800 s^{-1} upon blocking LFA-1.

In summary, these data demonstrate that primary bone marrow HSPCs, like KG1a cells, can migrate upstream on surfaces containing ICAM-1 and MAdCAM-1, and this upstream migration is dependent on LFA-1.

KG1a and HPSCs migrate upstream on HUVEC monolayers

Considering that both KG1a cells and HSPCs were able to migrate upstream on recombinant CAM surfaces, we tested whether KG1a and primary HSPCs exhibited upstream motility on primary HUVEC monolayers (Fig. 8). KG1a cells (Fig. 8A, left panel; Movie 8) primarily migrate against the direction of flow, and all upstream motion could be suppressed upon blocking the α_L integrin (Fig. 8A, middle panel) or enhanced further by blocking the α_4 integrin (Fig. 8A, right panel). This preference is also seen in the MI (Fig. 8C) and the percentage of cells migrating upstream (Fig. 8D) as the overall MI is upstream (−0.10±0.03) and 57.4% of cells migrate upstream in the presence of negative control isotype-

Journal of Cell Science (2018) 131, jcs205575. doi:10.1242/jcs.205575

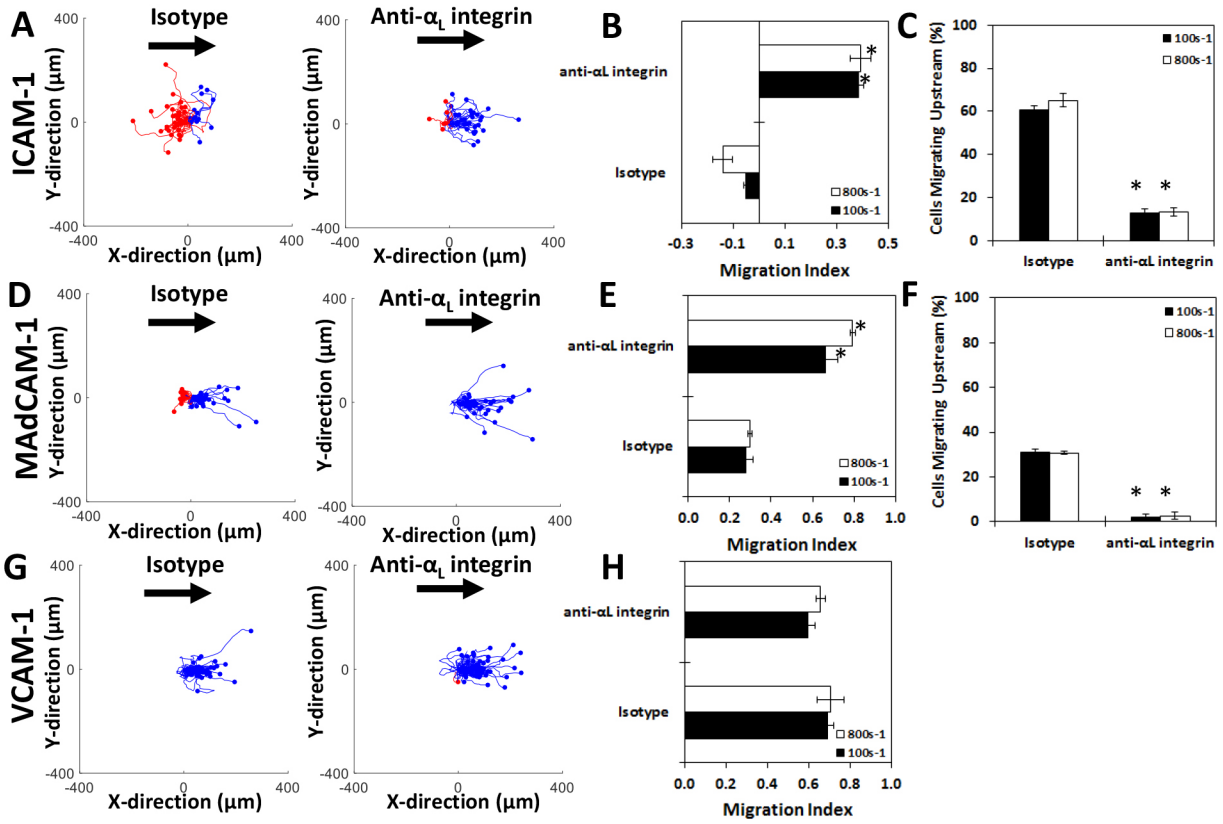

Fig. 6. Primary HSPCs show similar migration profiles to KG1a cells on ICAM-1, VCAM-1 and MAdCAM-1. Cell traces of bone marrow HSPCs on (A) ICAM-1, (D) MAdCAM-1 and (G) VCAM-1 under isotype (first column) or anti-α_L integrin blocking (second column) at a concentration of 5 µg/ml and an 800 s^{-1} shear rate. Traces are the cumulative tracks of two independent experiments and have units of µm. Blue traces indicate cells that traveled downstream (with flow), while red traces indicate cells that traveled upstream (against flow). The direction of flow is from left to right. In general, most traces indicate upstream migration on ICAM-1 and downstream migration on VCAM-1 while having bi-directionality on MAdCAM-1. The direction of HSPC migration under shear flow as expressed by the MI under isotype or anti-α_L integrin blocking at an 100 s^{-1} and 800 s^{-1} shear rate on (B) ICAM-1, (E) MAdCAM-1 or (H) VCAM-1. Percentage of migrating cells traveling upstream under isotype control or anti-α_L integrin blocking at 100 s^{-1} and 800 s^{-1} shear rate on (C) ICAM-1 or (F) MAdCAM-1. No cells migrated upstream on VCAM-1. More HSPCs migrate upstream on ICAM-1 as flow rate increases, migrate downstream on VCAM-1 and slightly downstream on MAdCAM-1, independently of flow rate. Blocking the α_L integrin of stops upstream migration on ICAM-1 and MAdCAM-1 surfaces while not affecting migration on VCAM-1. *n*=4–5 independent experiments of at least 40 cells analyzed per experiment for each CAM. **P*<0.05 with respect to isotype conditions (Student's *t*-test).

matched antibodies. Downstream migration could be induced (MI=0.52±0.05), with only 11.4% of cells migrating upstream, by blocking LFA-1. Blocking the α_4 integrin slightly increased upstream migration (MI=−0.19±0.01) with 71% of cells migrating upstream.

With HSPCs, blocking ICAM-1 or VCAM-1 on the HUVEC surface (Fig. S6) had similar effects to blocking the α_L integrin and the α_4 integrin, respectively. If ICAM-1 was blocked, only 8.9% of cells traveled upstream (MI=0.52±0.01). However, if VCAM-1 was blocked, 74.9% of cells traveled upstream (MI=−0.30±0.05). A substantial number of HSPCs were traveling upstream on HUVECs (Fig. 8B, left panel), although the upstream migration is not as pronounced as on molecularly pure surfaces. Like KG1a cells, all upstream motion could be removed upon blocking the α_L integrin (Fig. 8B, middle panel) or enhanced further (with KG1a cells) by blocking the α_4 integrin (Fig. 8B, right panel). The less pronounced, albeit still significant, upstream migration of HSPCs is also seen in the MI (Fig. 8C) and the percentage of cells migrating upstream (Fig. 8D), as the overall MI is downstream (0.25±0.04) and 34.7% of cells migrate upstream in the presence of negative control isotype-matched antibodies (as compared to a negative MI and >50% of cells migrating upstream with KG1a cells). Upon blocking LFA-1, the migration could be directed to almost completely downstream (MI=0.68±0.03) with only 3.8% of cells migrating upstream. Blocking the α_4 integrin significantly increased the upstream migration (MI=0.03±0.06) with 54.8% of cells migrating upstream. In summary, the data imply that upstream migration is a physiologically relevant phenomenon for primary bone marrow HSPCs, as they can migrate upstream on primary endothelial cells at shear rates seen *in vivo*.

DISCUSSION

Integrin interactions with endothelium-bound CAMs and subsequent migration under shear flow is one of the critical steps in the recruitment of immune cells to the sites of inflammation during the leukocyte adhesion cascade (Ley et al., 2007). HSPCs utilize this same pathway to migrate to the bone marrow microenvironment post transplantation where they re-establish hematopoiesis (Appelbaum, 2007; Sackstein, 2009). Much interest has been shown in understanding the trafficking of HSPCs in order to improve the ratio of cells injected that actually reach the bone marrow. In human stem cell transplants, a minimal dose of >2×10^6 cells/kg is recommended for rapid hematopoietic recovery (absolute neutrophil count >500/mm^3 for 3 consecutive

Journal of Cell Science (2018) 131, jcs205575. doi:10.1242/jcs.205575

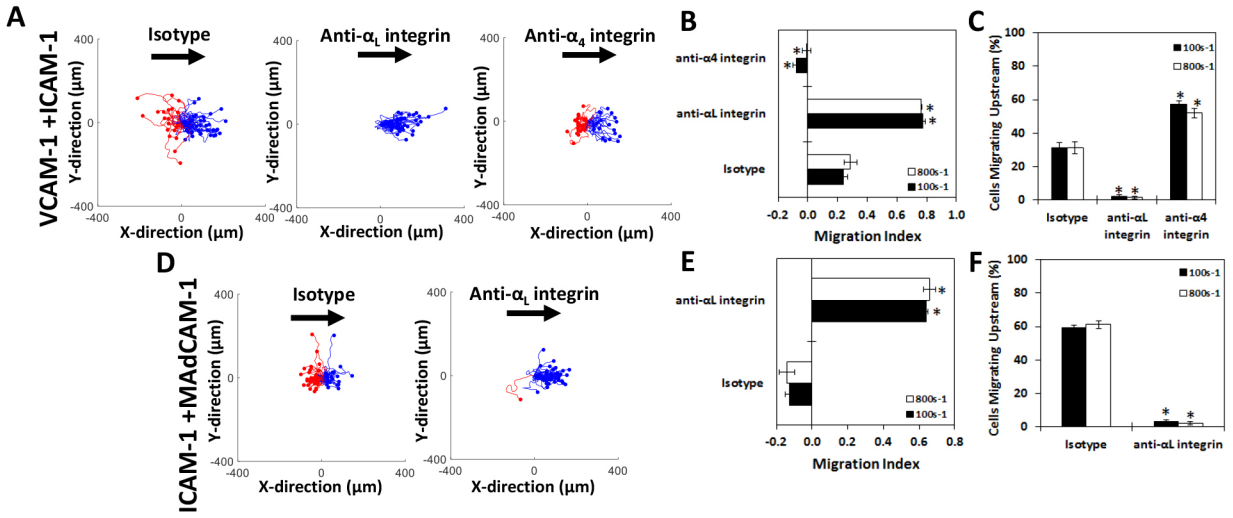

Fig. 7. Primary HSPCs behave similarly to KG1a cells on mixed CAM surfaces. Cell traces of bone marrow HSPCs on equal mixtures of (A) VCAM-1+ICAM-1 and (D) ICAM-1+MAdCAM-1 under isotype (first column), anti-α_L integrin blocking (second column) or anti-α_4 integrin blocking (third column) at a fixed concentration of 5 µg/ml and an 800 s^{-1} shear rate for the indicated surface preparations. The traces depicted are the cumulative tracks of two independent experiments and have units of µm. The direction of flow is from left to right in these traces. Most cell traces indicate travel downstream on VCAM-1+ICAM-1 surfaces and upstream on ICAM-1+MAdCAM-1. The direction of HSPC migration under shear flow as expressed by the MI under isotype or blocking conditions at 100 s^{-1} and 800 s^{-1} shear rate on (B) VCAM-1+ICAM-1 or (E) ICAM-1+MAdCAM-1. Percentage of migrating cells traveling upstream under isotype or blocking conditions at 100 s^{-1} and 800 s^{-1} shear rates on (C) VCAM-1+ICAM-1 or (F) ICAM-1+MAdCAM-1. HSPCs migrate upstream on combinations of both VCAM-1 +ICAM-1 and ICAM-1+MAdCAM-1 to varying degrees. Blocking the α_L integrin of stops upstream migration on both mixed surfaces while blocking the α_4 integrin of enhances upstream migration on the VCAM-1+ICAM-1 surface. *n*=4–5 independent experiments of at least 40 cells analyzed per experiment for each CAM. **P*<0.05 with respect to isotype conditions (one-way ANOVA for B,C; Students *t*-test E,F).

days; Bensinger et al., 1995). With only 1×10^8–2×10^8 transplantable HSPCs recovered from a normal apheresis product, the number of cells available for transplantation from a single donor is limited. Therefore, a better understanding of the mechanisms involved in HSPC homing will presumably improve patient outcomes post transplantation by allowing clinicians to deliver more HSPCs and aid in faster hematopoietic recovery.

While the main investigations of HSPC homing have focused on the mechanisms of the initial selectin-mediated interactions (Robinson et al., 2012; Sackstein, 2012) or upregulating the chemokine-mediated ‘inside-out’ activation (Kahn et al., 2003; Kollet et al., 2002; Peled et al., 1999b) of the integrins to allow the cell to better contact the endothelium, we focused on the biomechanics of HSPC migration under shear flow while in contact with surfaces presenting the three principal endothelial ligands: ICAM-1, VCAM-1 and MAdCAM-1 (Luster et al., 2005). Recent observations by ourselves and others have demonstrated that both murine (Steiner et al., 2010) and human (Valignat et al., 2013) T lymphocytes, but not neutrophils (Valignat et al., 2013), are able to efficiently crawl against the direction of shear flow on ICAM-1 surfaces as well as on surfaces with mixtures of ICAM-1 and VCAM-1, but crawl with the direction of flow on VCAM-1 substrates (Dominguez et al., 2015; Steiner et al., 2010). Here, we demonstrate that HSPCs also display the ability to migrate upstream under flow. Both the primitive immortalized KG1a cell line and bone marrow-derived HSPCs, which displayed a remarkably similar integrin ligand profile to T lymphocytes, could support upstream migration on surfaces containing ICAM-1 while maintaining a preference for downstream migration on VCAM-1 surfaces. In addition, we demonstrated the ability of KG1a cells and HSPCs to migrate in almost equal numbers in both directions, or bi-directionally, on MAdCAM-1.

Interesting differences in cell morphology were seen during migration as cells are predominantly rounded on VCAM-1, while on the ICAM-1 surfaces, cells have a mix of well-rounded cells and cells that look more spread out (Movies 1 and 6 for ICAM-1; Movies 2 and 7 for VCAM-1). Several differences between VLA-4–VCAM-1 and LFA-1–ICAM-1 migration could account for this observation. These include the fact that VLA-4 can bind to VCAM-1 at basal levels without stimulation to either of its active forms, while LFA-1 cannot bind to ICAM-1 in this manner. This may allow KG1a cells to bind to VCAM-1 without any inside-out signaling, which may cause more spreading along the surface. Furthermore, since these assays are performed in the absence of chemokines, this may account for the difference in morphology as VCAM-1 may need chemokine stimulation to induce spreading in a more fibroblast-like manner. As for migration on MAdCAM-1 surfaces, it is true that very few KG1a cells adhere to the surface and this is likely explained by the relatively low levels of the β_7 integrin chain (as compared to β_1 and β_2 integrin chains). Only ∼10 cells/mm^2 adhere to the MadCAM-1 surface (Fig. 4F) as compared to >200 and 60 cells/mm^2 for VCAM-1 and ICAM-1 surfaces, respectively. As for the HSPCs, in general many fewer cells interacted with the surface per frame. This is most likely due to the lower expression levels of β_1, β_2 and α_L integrin in HSPCs as compared to that in KG1a cells.

Experiments performed on surfaces with mixtures of two CAMs were even more enlightening as they elucidated what the directional preferences of the HSPCs were when presented with multiple CAMs. When combining VCAM-1 and ICAM-1 or ICAM-1 and MAdCAM-1, KG1a cells and HSPCs showed a net overall upstream migration on ICAM-1+MAdCAM-1 surfaces and a net overall downstream migration on VCAM-1+ICAM-1 surfaces. If as little as 25% of the surface is ICAM-1 in ICAM-1+MAdCAM-1 mixtures, the cells migrate upstream. The effect of MAdCAM-1 on migration

Journal of Cell Science (2018) 131, jcs205575. doi:10.1242/jcs.205575

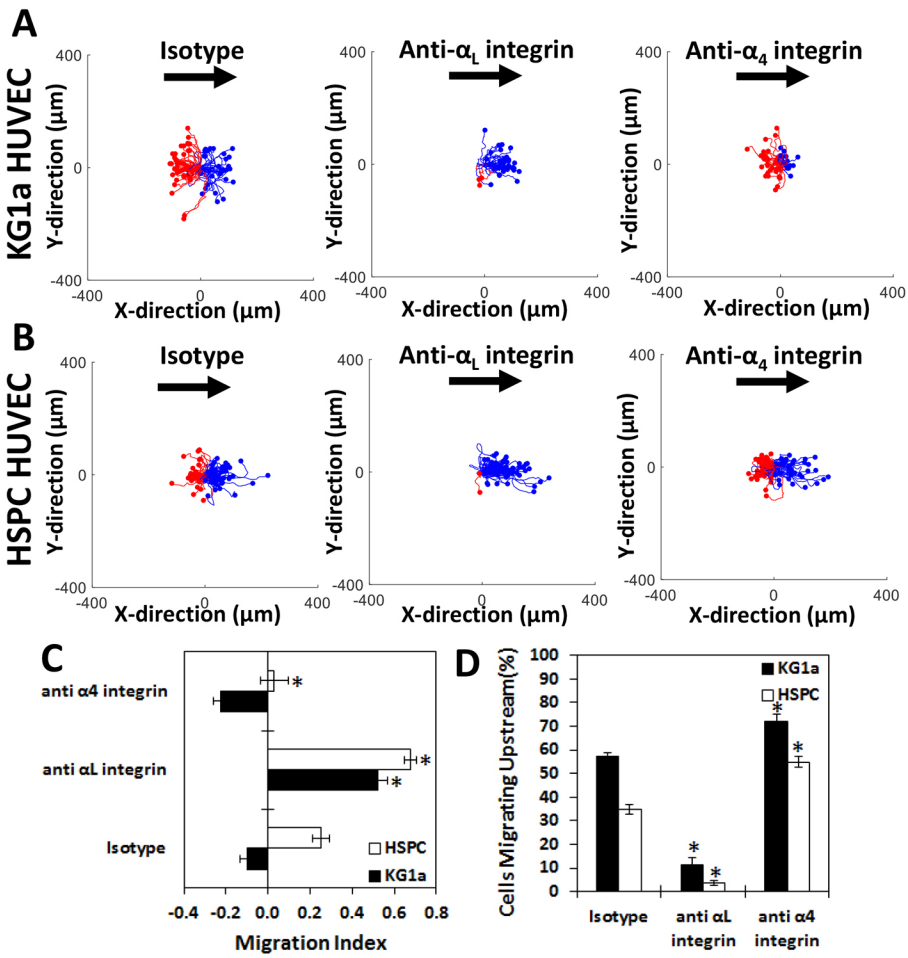

Fig. 8. KG1a cells and HSPCs migrate upstream on endothelial monolayers. Cell traces of (A) KG1a cells and (B) bone marrow HSPCs on IL-1β-stimulated HUVECs under isotype (first column), anti-α_L integrin blocking (second column) or with anti-α_4 integrin blocking (third column) at an 100 s^{-1} shear rate. The traces depicted are the cumulative tracks of two independent experiments and have units of μm. The direction of flow is from left to right. The direction of KG1a cell and HSPC migration under shear flow as expressed by the MI (C) or percentage of migrating KG1a cell and HSPCs traveling upstream (D) under isotype, anti-α_L integrin blocking or anti-α_4 integrin blocking at an 100 s^{-1} shear rate on HUVECs. Both KG1a cells and HSPCs migrate upstream on HUVECs to varying degrees and blocking the α_L integrin stops all upstream migration while blocking the α_4 integrin enhances it. *n*=4 independent experiments of at least 60 cells analyzed per experiment. **P*<0.05 with respect to isotype conditions (one-way ANOVA).

is not surprising, since both KG1a cells and HSPCs have a marginal expression of the MAdCAM-1 ligand LPAM-1 ($\alpha_4\beta_7$) (Berlin et al., 1993) compared to LFA-1 which binds to ICAM-1. In addition, LPAM-1 can sustain binding to MAdCAM-1 in its closed form (Briskin et al., 1996), which may account for the majority of the downstream interactions seen in the bi-directional motion on pure MAdCAM-1 surfaces. While upstream migration is seen on VCAM-1+ICAM-1 surfaces, KG1a cells and HSPCs switch to a downstream MI when the mixture contains 10% of is VCAM-1. This is the opposite of what is seen for T lymphocyte migration on VCAM-1+ICAM-1 surfaces, as T cells prefer to travel upstream on VCAM-1+ICAM-1 surfaces when any ICAM-1 is added to the surface (Dominguez et al., 2015). This distinction likely results from a difference in how integrins respond to CAM ligation in the two cell types. For example, in HSPCs, VCAM-1 dominates over ICAM-1 and selectins (Papayannopoulou et al., 2001) for homing to the bone marrow, while in contrast T lymphocytes are in constant contact with ICAM-1 surfaces during migration (Hogg et al., 2004). The VCAM-1+ICAM-1 surface is also of particular interest because it recapitulates the composition of the primary CAMs that are present on endothelium upon activation by TNF and IL-β during inflammation (MacKay et al., 1993). In addition, the ability to increase upstream migration of HSPCs on surfaces of mixed composition by blocking the α_4 integrin is interesting and has implications for anti-VLA4 therapies such as Natalizumab (Schwab et al., 2015). Furthermore, since our laboratory and others have shown that upstream migration is preserved on endothelial cells (Steiner et al., 2010), which display both ICAM-1 and VCAM-1, the net downstream migration of KG1a cells and HSPCs seen on the I_{50}+V_{50} surface may be due to some ligand that helps stabilize upstream migration that is lacking on the recombinant surface but preserved on the endothelial surface.

Our data also isolated LFA-1 as the critical cell-borne integrin controlling upstream migration. Blocking LFA-1 removed all upstream migration on surfaces made of the ICAM-1 or MAdCAM-1, and also surfaces that combine VCAM-1+ICAM-1 or ICAM-1+MAdCAM-1. In order to begin to understand how the cell reorganizes occurring during upstream and downstream migration, we performed fluorescence imaging to determine the localization of both the active forms (intermediate and high affinity conformations) of LFA-1 using the conformation-sensitive antibody KIM-127 (Fig. S4) and to image the F-actin network using KG1a cells transfected with GFP–Lifeact (Fig. S5). Our data demonstrate that the activated form of LFA-1 is found at the trailing edge and the uropod whenever the cell is crawling upstream (ICAM-1), whereas it is found in the lamellipod when moving cells are crawling downstream (as they do on VCAM-1 surfaces) (Fig. S4). Furthermore, the localization of F-actin was the the exact opposite, with GFP–Lifeact localized at the leading edge during upstream migration on ICAM-1 and at the trailing edge and the uropod during downstream migration on VCAM-1 surfaces (Fig. S5). Taken together, this points to critical differences in the integrin–actin complex during upstream and downstream migration, which warrants further study. Specifically, we are interested in how the reported crosstalk between the LFA-1 and VLA-4 integrins in both activating and inhibiting the function of each other (Chan et al.,

2000; Chigaev and Sklar, 2012; Grönholm et al., 2016) plays a role in governing upstream versus downstream migration, the integrin activation states and trafficking to the bone marrow post transplantation in HSPCs.

A previous study has put forth the hypothesis that the upstream migration of the T lymphocytes is due to a passive steering mechanism of the uropod during shear flow (Valignat et al., 2014). The 'wind-vane' hypothesis was borne from the few changes in upstream migration seen when intracellular Ca^{2+} signaling and phosphoinositide 3-kinase (PI3K) were inhibited, and the ability to change the direction of migration by repositioning the uropod using beads that could change the hydrodynamic drag, or magnetic beads that could be used to manipulate the direction of migration when in a magnetic field. Our work further implicates the uropod as critical as the cytoskeletal organization of F-actin and distribution of active LFA-1 in the uropod is fundamentally different based on the direction of motion. However, it was also found previously that the uropod is weakly adherent in T cells (Valignat et al., 2014) and additional imaging by interference reflection microscopy needs to be performed to assess the intimacy of contact of the uropod in HSPCs.

Nevertheless, this paper illustrates that the fascinating phenomenon of upstream migration of trafficking immune cells under flow, which was first observed in T-cells, also occurs in HSPCs. As has been suggested by others, upstream migration after initial binding may be a natural mechanism by which cells home back to their site of activation after arrest. Depending on the levels of adhesion molecule expression on the endothelium (Beste et al., 2012), it may take several seconds and considerable distances before a cell arrests downstream of the stimulatory site. Thus, upstream migration under flow may be a more universal mechanism of fine-tuning homing than has been previously thought. The ability to recreate this phenomenon in an immortalized cell line such as KG1a cells, which capture the essential essence of HSPCs and are amenable to genetic manipulation, opens future possibilities for elucidating the molecular mechanisms of upstream migration under flow.

In conclusion, the fact that KG1a cells and primary HSPCs undergo LFA-1-mediated upstream migration, like T-lymphocytes, is fascinating. Since upstream migration has been demonstrated under biologically relevant shear flow conditions, with primary HSPCs, and *in vitro* on activated HUVEC monolayers, further study is warranted to determine whether the upstream migration occurs with HSPCs *in vivo*. Although a specific biological function for upstream migration has yet to be elucidated, one can speculate that this unique mode of motility is beneficial for HSPC homing to the bone marrow post transplantation and that it can be leveraged for clinical benefit.

MATERIALS AND METHODS

Cell culture

All primary and cell lines were cultured as described previously (Lee et al., 2014; Mondal et al., 2014, 2016; Stolfa et al., 2016). Briefly, KG1a cells (ATCC) were cultured as described previously in Iscove's modified Eagle's medium (IMDM) containing 20% fetal bovine serum (FBS). Frozen aliquots of primary bone marrow HSPCs were obtained from the University of Pennsylvania Stem Cell and Xenograft Core. HSPCs were revived and cultured in Stemspan serum-free medium (Stem Cell Technologies, Vancouver, BC) overnight prior to experimentation (Dougher et al., 2017). Human umbilical vein endothelial cells (HUVECs) were maintained in EBM-2 growth medium with BulletKit supplement (Lonza, Wakersville, MD). For experimentation, HUVECs were seeded in a 35 mm×10 mm tissue culture treated dish (BD Falcon, Bedford, MA) and grown to confluence. HUVECs were then stimulated with IL-1β (BioLegend, San Diego, CA) for 4 h prior to experimentation.

Preparation of adhesion molecule-coated surfaces

Briefly, either TC treated 24-well plates (BD Falcon) for static experiments or 1 inch×3 inch plastic microscope slides (Fisher Scientific, Waltham, MA) for shear flow experiments were coated with 2 µg/ml Protein A/G (Biovision, Milpitas, CA) overnight at 4°C. Upon washing three times with 1× PBS, surfaces were treated with 0.2% Pluronic F127 (Sigma-Aldrich, St Louis, MO) for 1 h to block non-specific binding to the surface. After three additional 1× PBS washes, surfaces were the coated with a total concentration of 2.5 µg/ml of recombinant human ICAM-1 Fc, VCAM-1 Fc, MAdCAM-1 Fc (R&D Systems, Minneapolis, MN) or a mixture of these CAMs for 1 h. Human fibronectin surfaces (Sigma-Aldrich) were coated at a range of 2.5–100 µg/ml for 1 h at 37°C and then washed three times with 1× PBS. Surfaces were then treated with 0.2% pluronic acid F127 for 1 h and washed an additional three times with 1× PBS prior to experiments.

Static migration assays

After the preparation of either fibronectin or CAM-coated 24-well plates, 500 µl of IMDM+20% FBS was added to each experimental well. KG1a cells were then seeded at a concentration 5000 cells/cm^2 and allowed to settle and attach to the surface for 30 min. The plate was then mounted on a microscope in a 5% CO_2 and 37°C environment for 15 min to allow for equilibration. Images were captured every minute for 30 min on a motorized stage and observed using a Nikon Eclipse TE300 phase-contrast microscope. Images were captured using a 10× objective.

Flow chamber assembly and assay for recombinant surfaces

Experiments were conducted as described previously (Buffone et al., 2013, 2017). Briefly, a parallel-plate flow chamber (GlycoTech, Gaithersburg, MD) was used with a prepared plastic slide functionalized with either ICAM-1 Fc, VCAM-1 Fc, MAdCAM-1 Fc or mixtures of the CAMs. The channel template was cut from 0.01-inch-thick Duralastic sheeting (Allied Biomedical, Ventura, CA). For each flow experiment, the template was placed over the prepared slide. The template and slide were placed in the bottom well of the flow chamber, and the top was secured with screws. The chamber was assembled under water to minimize the introduction of air. It was then mounted on the microscope in a 5% CO_2 and 37°C environment for 10 min to allow for equilibration. Before introduction of cells, the chamber was flushed with running medium (IMDM). A volume of 2 ml containing 10^6 cells in running medium was introduced into the chamber and cells were allowed to attach for 30 min in which time most but not all migrating cells adopt a polarized morphology consisting of a lamellipod at the front and a uropod at the rear. These actively migrating cells were the cells included in the analysis. The overall morphology of cells varied as both KG1a cells and HSPCs are a heterogeneous population of cells but the majority of spherical and non-adherent cells were either washed away upon application of flow or demonstrated no motility and were not included in the analysis. Fluid flow was initiated by using a syringe pump (11 Plus, Harvard Apparatus, Holliston, MA) and volumetric flow rates were adjusted accordingly to correspond to desired shear rates. Shear rate was calculated using $\tau_w=(6\,\mu Q)/(h^2 w)$ where μ is the fluid viscosity, Q is the volumetric flow rate, h is the channel height and w is the channel width. For this chamber, h=0.023 cm and w=0.1 cm. Images were captured every minute on a motorized stage of a Nikon Eclipse TE300 phase-contrast microscope. Images were captured using a 10× objective. The number of cells per mm^2 was calculated as the average of the number of cells migrating at six unique positions in the chamber and normalizing this average per mm^2.

Shear assays on stimulated HUVEC surfaces

Experiments were conducted under similar conditions to those in previous studies (MacKay and Hammer, 2016; Mondal et al., 2014). In brief, HUVECs (Lonza) were seeded and grown to confluence in EGM-2 medium with Bullet supplements (Lonza) on 35×10 mm tissue culture treated polystyrene plates (BD Falcon) and gown to near confluence at 37°C and 5% CO_2. Prior to experimentation, HUVECs were supplied with fresh EGM-2 medium supplemented with 10 ng/ml recombinant IL-1β (BioLegend) and allowed to incubate for a minimum of 4 h to ensure robust expression of E-selectin, ICAM-1 and VCAM-1 on the surface. To perfuse the KG1a cells

and HSPCs across the HUVEC monolayer, we used a circular parallel-plate flow chamber (Glycotech 31-001) under vacuum, fitted with a rubber gasket to create a rectangular flow path (h=127µm, w=0.25 cm). The chamber was assembled under water to minimize the introduction of air. It was then mounted on the microscope in a 5% CO_2 and 37°C environment for 10 min to allow for equilibration. Before introduction of cells, the chamber was flushed with running medium (IMDM). A volume of 2 ml containing 10^6 cells in running medium was introduced into the chamber and cells were allowed to attach for 30 min. From this point on, the assay was performed under similar conditions to the previous experiments on recombinant surfaces as described above.

Antibody blocking

Functional blocking antibodies HL111 (anti-CD11a/α_L integrin; cat. no 301214), 3.9 (anti-CD11c/α_X integrin; cat. no 301616), 9F10 (anti-CD49d/α_4 integrin; cat. no 103718), DREG-56 (anti-CD62L; cat. no 304812), HCD54 (anti-CD54/ICAM-1; cat. no 322704), HAE-1F (anti-CD62E/E-selectin; cat. no 336004), and FIB27 (anti-β_7 integrin; cat. no 121003) from BioLegend and HUTS-21 (anti-CD29/β_1 integrin; cat. no 556048), L130 (anti-CD18/β_2 integrin; cat. no 556084), and 51-10C9 (anti-CD106/VCAM-1; cat. no 556645) were obtained from BD Biosciences, San Jose, CA. 5×10^5 KG1a cells or HSPCs were blocked with a final concentration of 50 µg/ml blocking antibody in 25 µl running medium and incubated for 30 min at 37°C and 5% CO_2 as described previously (MacKay and Hammer, 2016). Cells were then injected into flow chamber apparatus and allowed to adhere in the absence of flow for 30 min. Running buffer consisted of IMDM and a 1:10 final antibody blocking concentration. Cells were exposed to flow for 30 min before quantification of speed and MI.

Measurement of cell trajectories, speed and MI

Cell movement was tracked using the ImageJ plugin Manual Tracking as described previously (Dominguez et al., 2015). ImageJ and the plugin are both freely available through the NIH website (http://rsbweb.nih.gov/ij/). The centroid of the cell was considered to represent the cell position. Time-lapse microscopy was used and images were taken every minute. The result was a series of (x_i,y_i) positions with time for each cell. The net displacement during the ith minute increment, D_i, was calculated by determining the difference of the position at the beginning and end of the time step. The sum of total displacements ($D_{i,accum}$) was used to calculate the cell speed over the entire experimental time course of 30 min. The MI was defined as the ratio of the difference between the initial and final x-displacement to total displacement where $MI=(x_{i,end}-x_{i,initial})/(D_{i,accum})$. Values of the MI near −1, indicate that cells migrate in a straight trajectory against the direction of flow while values near +1, indicate migration in a straight trajectory in the direction of flow. When the MI is near 0, there is no preferred direction in migration, indicating random motility. Only single cells actively migrating along the surface which remained in the field of view for the entire experiment were included in the analysis. Dividing cells and clusters of cells in which the cells interacted with one another's path were not included in analysis, and neither were stationary cells or loosely adhered cells.

Flow cytometric profiling of inflammatory cells

Immunofluorescence staining and flow cytometric analysis of cells were performed as described previously (Buffone et al., 2013). Cells (0.5×10^6–1×10^6) were washed in PBS twice before labeling. Samples were incubated with combinations of fluorescently labeled antibodies HI111 (anti-CD11a/LFA-1; cat. no 301206), ICRF44 (anti–CD11b/Mac-1; cat. no 301330), 3.9 (anti-CD11c; cat. no 301604), DREG-56 (anti-CD62L/L-selectin; cat. no 304608), 561 (anti-CD34; cat. no 343604), HB-7 (anti-CD38; cat. no 356606), 9F10 (anti-CD49d; cat. no 304316), NKI-SAM-1 (anti-CD49e; cat. no 328008), TS1/18 (anti-CD18/β_2-integrin; cat. no 302106), TS2/16 (anti-CD29/β_1-integrin; cat. no 303016), and FIB27 (anti-β_7-integrin; cat. no 121010) for 15 min before analysis. All antibodies were from Biolegend (San Diego, CA). Flow cytometric analysis was performed with a Calibur flow cytometer (Becton Dickinson Immunocytometry Systems, Franklin Lakes, NJ) and the FACS Diva software package and histograms were generated using the FlowJo software.

Staining and immunofluorescence

Parallel flow chamber assays were performed as described above and previously (Dominguez et al., 2015). Upon completion of experiments, the cells were fixed with 4% paraformaldehyde in PBS for 7 min that was flowed through at the experimental shear rate. The substrate was removed from the flow chamber apparatus and then blocked with 1% bovine serum albumin (BSA) in PBS for 30 min at room temperature. Cells were incubated with 1:1000 Alexa Fluor 568-labeled anti-LFA-1 intermediate affinity clone KIM-127 for 30 min at room temperature followed by DAPI for a subsequent 30 min. Cells were mounted in Fluoromount-G mounting medium (SouthernBiotech, Birmingham, AL) and examined by confocal microscopy (Leica SP5).

Expression of GFP–Lifeact in KG1a cells

Recombinant lentivirus was produced as described previously (Buffone et al., 2013; Mondal et al., 2014) by transfecting 15 µg psPAX2 (Addgene plasmid #12260), 10 µg pMD2.G (Addgene plasmid #12259) and 20 µg pLX301 (Addgene plasmid #25895; Yang et al., 2011) modified to contain GFP–Lifeact into HEK239T (ATCC, Manassas, VA) cells through calcium phosphate precipitation. 5×10^6 cells KG1a cells were mixed with harvested 100× lentiviral suspension, spun at 1200 ***g*** for 2 h, and re-suspended in fresh culture medium. After 48 h, GFP–Lifeact-positive cells were selected with 2.5 µg/ml puromycin (Sigma) and later verified by fluorescence microscopy.

Statistics

Data are presented as mean±s.e.m. Testing for differences between means was determined with either Student's t-test or two-way ANOVA with post hoc comparisons in InStat 3 software (GraphPad, San Diego, CA). $P<0.05$ was considered significant. P-values are indicated in figure legends.

Acknowledgements

The authors would like to thank Dr Nathan Roy and Prof. Janis Burkhardt (Children's Hospital of Philadelphia) for the KG1a GFP–Lifeact cells and Prof. Donna Wall (The Hospital for Sick Children) for her helpful discussions regarding the clinical impacts of HSPC homing.

Competing interests

The authors declare no competing or financial interests.

Author contributions

Conceptualization: D.A.H., A.B.; Methodology: D.A.H., A.B., N.A.; Validation: A.B.; Formal analysis: A.B.; Investigation: A.B.; Resources: N.A.; Writing - original draft: A.B.; Writing - review & editing: D.A.H., A.B., N.A.; Supervision: D.A.H.; Project administration: D.A.H.; Funding acquisition: D.A.H.

Funding

This work was supported by the National Institutes of Health (grants AI082292 and GM123019) to D.A.H. Deposited in PMC for release after 12 months.

Supplementary information

Supplementary information available online at
http://jcs.biologists.org/lookup/doi/10.1242/jcs.205575.supplemental

References

Appelbaum, F. R. (2007). Hematopoietic-cell transplantation at 50. *N. Engl. J. Med.* **357**, 1472-1475.

Bensinger, W., Appelbaum, F., Rowley, S., Storb, R., Sanders, J., Lilleby, K., Gooley, T., Demirer, T., Schiffman, K. and Weaver, C. (1995). Factors that influence collection and engraftment of autologous peripheral-blood stem cells. *J. Clin. Oncol.* **13**, 2547-2555.

Berlin, C., Berg, E. L., Briskin, M. J., Andrew, D. P., Kilshaw, P. J., Holzmann, B., Weissman, I. L., Hamann, A. and Butcher, E. C. (1993). α4β7 integrin mediates lymphocyte binding to the mucosal vascular addressin MAdCAM-1. *Cell* **74**, 185-195.

Beste, M. T., Lee, D., King, M. R., Koretzky, G. A. and Hammer, D. A. (2012). An integrated stochastic model of "inside-out" integrin activation and selective T Lymphocyte recruitment. *Langmuir* **28**, 2225-2237.

Briskin, M. J., Rott, L. and Butcher, E. C. (1996). Structural requirements for mucosal vascular addressin binding to its lymphocyte receptor α4β7: common themes among integrin-Ig family interactions. *J. Immunol.* **156**, 719-726.

Buffone, A., Mondal, N., Gupta, R., McHugh, K. P., Lau, J. T. Y. and Neelamegham, S. (2013). Silencing α1,3-fucosyltransferases in human leukocytes reveals a role for FUT9 enzyme during E-selectin-mediated cell adhesion. *J. Biol. Chem.* **288**, 1620-1633.

Buffone, A., Nasirikenari, M., Manhardt, C. T., Lugade, A., Bogner, P. N., Sackstein, R., Thanavala, Y., Neelamegham, S. and Lau, J. T. Y. (2017). Leukocyte-borne α(1,3)-fucose is a negative regulator of β2-integrin-dependent recruitment in lung inflammation. *J. Leukoc. Biol.* **101**, 459-470.

Carvalho, J. M., Souza, M. K., Buccheri, V., Rubens, C. V., Kerbauy, J. and Oliveira, J. S. R. (2009). CD34-positive cells and their subpopulations characterized by flow cytometry analyses on the bone marrow of healthy allogenic donors. *Sao Paulo Med. J.* **127**, 12-18.

Chan, J. Y.-H. and Watt, S. M. (2001). Adhesion receptors on haematopoietic progenitor cells. *Br. J. Haematol.* **112**, 541-557.

Chan, J. R., Hyduk, S. J. and Cybulsky, M. I. (2000). α4β1 integrin/VCAM-1 interaction activates αLβ2 integrin-mediated adhesion to ICAM-1 in human T cells. *J Immunol.* **164**, 746-753.

Chigaev, A. and Sklar, L. (2012). Aspects of VLA-4 and LFA-1 regulation that may contribute to rolling and firm adhesion. *Front. Immunol.* **3**, 242.

Dimitroff, C. J., Lee, J. Y., Rafii, S., Fuhlbrigge, R. C. and Sackstein, R. (2001a). Cd44 is a major E-selectin ligand on human hematopoietic progenitor cells. *J. Cell Biol.* **153**, 1277-1286.

Dimitroff, C. J., Lee, J. Y., Schor, K. S., Sandmaier, B. M. and Sackstein, R. (2001b). Differential L-selectin binding activities of human hematopoietic cell L-selectin ligands, HCELL and PSGL-1. *J. Biol. Chem.* **276**, 47623-47631.

Dominguez, G. A., Anderson, N. R. and Hammer, D. A. (2015). The direction of migration of T-lymphocytes under flow depends upon which adhesion receptors are engaged. *Integr. Biol.* **7**, 345-355.

Dougher, C. W. L., Buffone, A., Nemeth, M. J., Nasirikenari, M., Irons, E. E., Bogner, P. N. and Lau, J. T. Y. (2017). The blood-borne sialyltransferase ST6Gal-1 is a negative systemic regulator of granulopoiesis. *J. Leukoc. Biol.* **102**, 507-516.

Greenberg, A. W., Kerr, W. G. and Hammer, D. A. (2000). Relationship between selectin-mediated rolling of hematopoietic stem and progenitor cells and progression in hematopoietic development. *Blood* **95**, 478-486.

Grönholm, M., Jahan, F., Bryushkova, E. A., Madhavan, S., Aglialoro, F., Soto Hinojosa, L., Uotila, L. M. and Gahmberg, C. G. (2016). LFA-1 integrin antibodies inhibit leukocyte α4β1–mediated adhesion by intracellular signaling. *Blood* **128**, 1270.

Hogg, N., Smith, A., McDowall, A., Giles, K., Stanley, P., Laschinger, M. and Henderson, R. (2004). How T cells use LFA-1 to attach and migrate. *Immunol. Lett.* **92**, 51-54.

Huttenlocher, A. and Horwitz, A. R. (2011). Integrins in cell migration. *Cold Spring Harbor Perspect. Biol.* **3**, a005074.

Kahn, J., Byk, T., Jansson-Sjostrand, L., Petit, I., Shivtiel, S., Nagler, A., Hardan, I., Deutsch, V., Gazit, Z., Gazit, D. et al. (2003). Overexpression of CXCR4 on human CD34+ progenitors increases their proliferation, migration, and NOD/SCID repopulation. *Blood* **103**, 2942-2949.

Katayama, Y., Hidalgo, A., Peired, A. and Frenette, P. S. (2004). Integrin α4β7 and its counterreceptor MAdCAM-1 contribute to hematopoietic progenitor recruitment into bone marrow following transplantation. *Blood* **104**, 2020-2026.

Kollet, O., Petit, I., Kahn, J., Samira, S., Dar, A., Peled, A., Deutsch, V., Gunetti, M., Piacibello, W., Nagler, A. et al. (2002). Human CD34+CXCR4− sorted cells harbor intracellular CXCR4, which can be functionally expressed and provide NOD/SCID repopulation. *Blood* **100**, 2778-2786.

Lee, M. M., Nasirikenari, M., Manhardt, C. T., Ashline, D. J., Hanneman, A. J., Reinhold, V. N. and Lau, J. T. Y. (2014). Platelets support extracellular sialylation by supplying the sugar donor substrate. *J. Biol. Chem.* **289**, 8742-8748.

Ley, K., Laudanna, C., Cybulsky, M. I. and Nourshargh, S. (2007). Getting to the site of inflammation: the leukocyte adhesion cascade updated. *Nat. Rev. Immunol.* **7**, 678-689.

Luster, A. D., Alon, R. and von Andrian, U. H. (2005). Immune cell migration in inflammation: present and future therapeutic targets. *Nat. Immunol.* **6**, 1182-1190.

MacKay, J. L. and Hammer, D. A. (2016). Stiff substrates enhance monocytic cell capture through E-selectin but not P-selectin. *Integr. Biol.* **8**, 62-72.

Mackay, F., Loetscher, H., Stueber, D., Gehr, G. and Lesslauer, W. (1993). Tumor necrosis factor alpha (TNF-alpha)-induced cell adhesion to human endothelial cells is under dominant control of one TNF receptor type, TNF-R55. *J. Exp. Med.* **177**, 1277-1286.

Mondal, N., Buffone, A., Stolfa, G., Antonopoulos, A., Lau, J. T. Y., Haslam, S. M., Dell, A. and Neelamegham, S. (2014). ST3Gal-4 is the primary sialyltransferase regulating the synthesis of E-, P-, and L-selectin ligands on human myeloid leukocytes. *Blood* **125**, 687-696.

Mondal, N., Stolfa, G., Antonopoulos, A., Zhu, Y., Wang, S.-S., Buffone, A., Atilla-Gokcumen, G. E., Haslam, S. M., Dell, A. and Neelamegham, S. (2016). Glycosphingolipids on human myeloid cells stabilize E-selectin–dependent rolling in the multistep leukocyte adhesion cascade. *Arterioscler. Thromb. Vasc. Biol.* **36**, 718-727.

Papayannopoulou, T., Craddock, C., Nakamoto, B., Priestley, G. V. and Wolf, N. S. (1995). The VLA4/VCAM-1 adhesion pathway defines contrasting mechanisms of lodgement of transplanted murine hemopoietic progenitors between bone marrow and spleen. *Proc. Natl Acad. Sci. USA* **92**, 9647-9651.

Papayannopoulou, T., Priestley, G. V., Nakamoto, B., Zafiropoulos, V. and Scott, L. M. (2001). Molecular pathways in bone marrow homing: dominant role of α4β1 over β2-integrins and selectins. *Blood* **98**, 2403.

Peled, A., Grabovsky, V., Habler, L., Sandbank, J., Arenzana-Seisdedos, F., Petit, I., Ben-Hur, H., Lapidot, T. and Alon, R. (1999a). The chemokine SDF-1 stimulates integrin-mediated arrest of CD34+ cells on vascular endothelium under shear flow. *J. Clin. Invest.* **104**, 1199-1211.

Peled, A., Petit, I., Kollet, O., Magid, M., Ponomaryov, T., Byk, T., Nagler, A., Ben-Hur, H., Many, A., Shultz, L. et al. (1999b). Dependence of human stem cell engraftment and repopulation of NOD/SCID mice on CXCR4. *Science* **283**, 845-848.

Robinson, S. N., Simmons, P. J., Thomas, M. W., Brouard, N., Javni, J. A., Trilok, S., Shim, J.-S., Yang, H., Steiner, D., Decker, W. K. et al. (2012). Ex vivo fucosylation improves human cord blood engraftment in NOD-SCID IL-2Rγnull mice. *Exp. Hematol.* **40**, 445-456.

Sackstein, R. (2009). Glycosyltransferase-programmed stereosubstitution (GPS) to create HCELL: engineering a roadmap for cell migration. *Immunol. Rev.* **230**, 51-74.

Sackstein, R. (2012). Glycoengineering of HCELL, the human bone marrow homing receptor: sweetly programming cell migration. *Ann. Biomed. Eng.* **40**, 766-776.

Sackstein, R. and Dimitroff, C. J. (2000). A hematopoietic cell L-selectin ligand that is distinct from PSGL-1 and displays N-glycan–dependent binding activity. *Blood* **96**, 2765-2774.

Sahin, A. O. and Buitenhuis, M. (2012). Molecular mechanisms underlying adhesion and migration of hematopoietic stem cells. *Cell Adh. Migr.* **6**, 39-48.

Schwab, N., Schneider-Hohendorf, T. and Wiendl, H. (2015). Therapeutic uses of anti-α4-integrin (anti-VLA-4) antibodies in multiple sclerosis. *Int. Immunol.* **27**, 47-53.

Schweitzer, K. M., Dräger, A. M., van der Valk, P., Thijsen, S. F., Zevenbergen, A., Theijsmeijer, A. P., van der Schoot, C. E. and Langenhuijsen, M. M. (1996). Constitutive expression of E-selectin and vascular cell adhesion molecule-1 on endothelial cells of hematopoietic tissues. *Am. J. Pathol.* **148**, 165-175.

She, M., Niu, X., Chen, X., Li, J., Zhou, M., He, Y., Le, Y. and Guo, K. (2012). Resistance of leukemic stem-like cells in AML cell line KG1a to natural killer cell-mediated cytotoxicity. *Cancer Lett.* **318**, 173-179.

Springer, T. A. (1994). Traffic signals for lymphocyte recirculation and leukocyte emigration: The multistep paradigm. *Cell* **76**, 301-314.

Steiner, O., Coisne, C., Cecchelli, R., Boscacci, R., Deutsch, U., Engelhardt, B. and Lyck, R. (2010). Differential roles for endothelial ICAM-1, ICAM-2, and VCAM-1 in shear-resistant T cell arrest, polarization, and directed crawling on blood–brain barrier endothelium. *J. Immunol.* **185**, 4846-4855.

Stolfa, G., Mondal, N., Zhu, Y., Yu, X., Buffone, A. and Neelamegham, S. (2016). Using CRISPR-Cas9 to quantify the contributions of O-glycans, N-glycans and Glycosphingolipids to human leukocyte-endothelium adhesion. *Sci. Rep.* **6**, 30392.

Valignat, M.-P., Theodoly, O., Gucciardi, A., Hogg, N. and Lellouch, A. C. (2013). T lymphocytes orient against the direction of fluid flow during LFA-1-mediated migration. *Biophys. J.* **104**, 322-331.

Valignat, M.-P., Nègre, P., Cadra, S., Lellouch, A. C., Gallet, F., Hénon, S. and Theodoly, O. (2014). Lymphocytes can self-steer passively with wind vane uropods. *Nat. Commun.* **5**, 5213.

Yang X, Boehm JS, Yang X, Salehi-Ashtiani K, Hao T, Shen Y, Lubonja R, Thomas SR, Alkan O, Bhimdi T et al.. (2011). A public genome-scale lentiviral expression library of human ORFs. **8**, 659-661.